공학석사학위논문

가스터빈 동익 캐스케이드 내 팁 간극에 따른 공력 성능에 대한 실험적 연구

Experimental Investigation of Aerodynamic Performance due to Tip Clearance in a Gas Turbine Rotor Cascade

2022 년 8 월

서울대학교 대학원

기계공학부

정 진 무

가스터빈 동익 캐스케이드 내 팁 간극에 따른 공력 성능에 대한 실험적 연구

Experimental Investigation of Aerodynamic Performance due to Tip Clearance in a Gas Turbine Rotor Cascade

지도교수 황 원 태

이 논문을 공학석사 학위논문으로 제출함

2022 년 4 월

서울대학교 대학원

기계공학부

정 진 무

정 진 무의 공학석사 학위논문을 인준함

2022 년 6 월

위 원 장 : 송성진 (인)

부위원장 : 황원태 (인)

위 원 : 김호영 (인)

Abstract

This study examines how the complex flow structure within a gas turbine rotor affects aerodynamic loss. An unshrouded linear turbine cascade was built, and velocity and pressure fields were measured using a 5-hole probe. In order to elucidate the effect of tip clearance and Reynolds number, the overall aerodynamic loss was evaluated by examining the total pressure field for each case. The tip clearance was varied from 0% to 4.2% of blade span and the chord length based Reynolds number was varied from 1.7 x 10^5 to 2.3 x 10^5.

For the case without tip clearance, a wake downstream of the blade trailing edge is observed, along with hub and tip passage vortices. These flow structures result in profile loss at the center of the blade span, and passage vortex related losses towards the hub and tip. As the tip clearance increases, a tip leakage vortex is formed, and it becomes stronger and eventually alters the tip passage vortex. Because of the interference of the secondary tip leakage flow with the main flow, the streamwise velocity decreases while the total pressure loss increases significantly by tenfold in the last 30% blade span region towards the tip for the 4.2% tip clearance case.

It was additionally observed that the overall aerodynamic loss increases linearly with tip clearance. On the other hand, the effect by Reynolds number increased the streamwise velocity, but

change in flow structure and aerodynamic loss was insignificant.

Keyword : gas turbine, rotor cascade, aerodynamic loss, tip clearance, Reynolds number

Student Number : 2020-25852

Table of Contents

Abstract i

Table of Contents iii

List of Figures v

List of Tables vii

Nomenclature viii

Chapter 1. Introduction 1

1.1 Study Background 1

1.2 Purpose of Research 3

Chapter 2. Experimental Facility and Method 4

2.1 Turbine Rotor Linear Cascade 4

2.2 Experimental Conditions 6

2.3 Instrumentation 8

2.4 Experimental Uncertainty 10

2.5 Static Pressure Periodicity 11

Chapter 3. Results of Tip Clearance Effects 13

3.1 Downstream Flow Structure 13

3.2 Streamwise Velocity Distribution 15

3.3 Total Pressure Loss Coefficient Distribution.....17

3.4 Pitch-wise Mass Averaged Loss Coefficient 19

3.5 Overall Mass Averaged Loss Coefficient 22

Chapter 4. Results of Reynolds Number Effects 25

4.1 Downstream Flow Structure 25

4.2 Streamwise Velocity Distribution 27

4.3 Total Pressure Loss Coefficient Distribution.....29

4.4 Pitch-wise Mass Averaged Loss Coefficient 31

4.5 Overall Mass Averaged Loss Coefficient 33

Chapter 5. Conclusions 35

Acknowledgements..... 37

Bibliography..... 38

Abstract in Korean 41

List of Figures

Fig. 1 5

Fig. 2 5

Fig. 3 6

Fig. 4 8

Fig. 5 9

Fig. 6 12

Fig. 7 14

Fig. 8 16

Fig. 9 18

Fig. 10 21

Fig. 11 24

Fig. 12..... 26

Fig. 13..... 28

Fig. 14..... 30

Fig. 15..... 32

Fig. 16..... 34

List of Tables

Table 1..... 7

Table 2..... 23

Table 3..... 24

Table 4..... 34

Nomenclature

Nomenclature	
c	chord length/mm
C_p	static pressure coefficient
H	cascade height/mm
p	blade pitch/mm
P_s	static pressure/Pa
P_t	total pressure/Pa
PS	pressure side
Re	Reynolds number
s	blade span/mm
SS	suction side
U	streamwise velocity/m · s^{-1}
y	spanwise distance/mm
Y	total pressure loss coefficient
z	pitchwise distance/mm

Greek symbols	
α	inlet blade angle/°
β	outlet blade angle/°
ρ	flow density/kg · m^{-3}
τ	tip clearance/mm
Δ	tip clearance loss

Subscripts

0	zero tip clearance case
∞	ambient value
in	inlet
out	outlet

Chapter 1. Introduction

1.1. Study Background

Many studies have conducted aerodynamic performance analysis to improve the efficiency of gas turbines. As a rotating power engine, a gas turbine inevitably has a gap between the rotor blade tip and casing, which is an important factor affecting the aerodynamic efficiency. Due to this tip clearance, a significant change in flow path occurs at the blade tip, a typical example being the tip leakage flow from the pressure side of the blade to the suction side due to pressure difference. This leakage flow reduces the blade downstream total pressure in the tip region, and results in a significant loss in aerodynamic performance.

There is a wide variety of existing blade shapes and operating conditions, and thus research on tip clearance continues to be actively conducted. Bindon [1] phenomenologically interpreted the complex flow caused by the tip clearance, identified the process and cause of the flow, and analyzed the loss caused by it. In addition, not only the limitations and alternatives of the study were specified, but the direction of future research for loss reduction was presented. Nho et al. [2] experimentally investigated the secondary flow structure and total pressure loss in a low speed turbine cascade by varying blade tip shape. Wang et al. [3] numerically evaluated the effects of tip leakage flow due to tip clearance at transonic conditions. These groups presented

qualitatively similar results by analysing the flow downstream of the blade, and confirmed that stronger tip leakage flow causes a reduction in aerodynamic performance. However, quantitatively the results are not the same due to the large differences in flow conditions. Yamamoto [4-5] examined flow characteristics and confirmed differences according to flow angle. Various loss models due to tip clearance have also been proposed [6-8], starting with the study of Ainley and Mathieson [8]. Persson [9] built a turbine simulation setup and applied these computationally.

Various previous studies have utilized a wind tunnel cascade to examine the effect of tip clearance. The flow and related losses were measured in the tip gap region for a large-scale turbine by Sjolander and Cao [10]. Williams et al. [11] analyzed the effects of large tip clearance in a linear cascade using both experimental and computational methods. Matsunuma [12] investigated flow characteristics downstream of the blade and the resulting aerodynamic loss according to the presence or absence of tip clearance for different Reynolds numbers and freestream turbulence intensity. Bi et al. [13] and Tallman and Lakshminarayana [14] conducted numerical studies to investigate the effects of tip clearance for a NACA0009 airfoil and an axial flow turbine, respectively.

Most of the related experiments have utilized linear cascades ignoring the relative motion of the casing and blade occurring in the actual turbine. The influence of relative motion by this rotation and in the absence of rotation has been examined

experimentally [14−16]. In addition, experimental results by rotation were compared with computational analysis [17−19]. This relative motion weakens the tip leakage flow, reducing the aerodynamic loss. However, this does not significantly affect the flow structure caused by the tip clearance.

1.2. Purpose of Research

This study aims to contribute to the improvement of gas turbine aerodynamic performance by assessing how the flow structure affects the aerodynamic loss caused by blade tip clearance and Reynolds number. First, a turbine rotor linear cascade was constructed, and periodicity of the flow at the blade exit plane was confirmed. Next, the flow structure was measured and the associated aerodynamic performance was investigated according to the variation of tip clearance and Reynolds number.

Chapter 2. Experimental Facility and Method

2.1. Turbine Rotor Linear Cascade

In this study, the flow from a wind tunnel (Fig. 1) enters a linear cascade with a spanwise height of 180 mm, as shown in Fig. 2. The boundary layer of the flow is removed in the boundary layer bleed region due to a height difference in the tunnel, in order to have uniform flow entering the cascade to ensure zero loss at the entry. A total of six blade passages were installed using seven blades, and experiments were conducted mainly in the central two passages. A 5-hole probe was inserted into the upper slot downstream of the blades (approximately 1.3 chord length from the blade leading edge) to measure the flow in the pitch and span directions. In addition, 25 static pressure holes are arranged at an interval of 16 mm at the bottom hub surface of the measurement location. By adjusting the tailboard angle, periodicity of static pressure could be established downstream of the blades.

Fig. 1. Wind tunnel

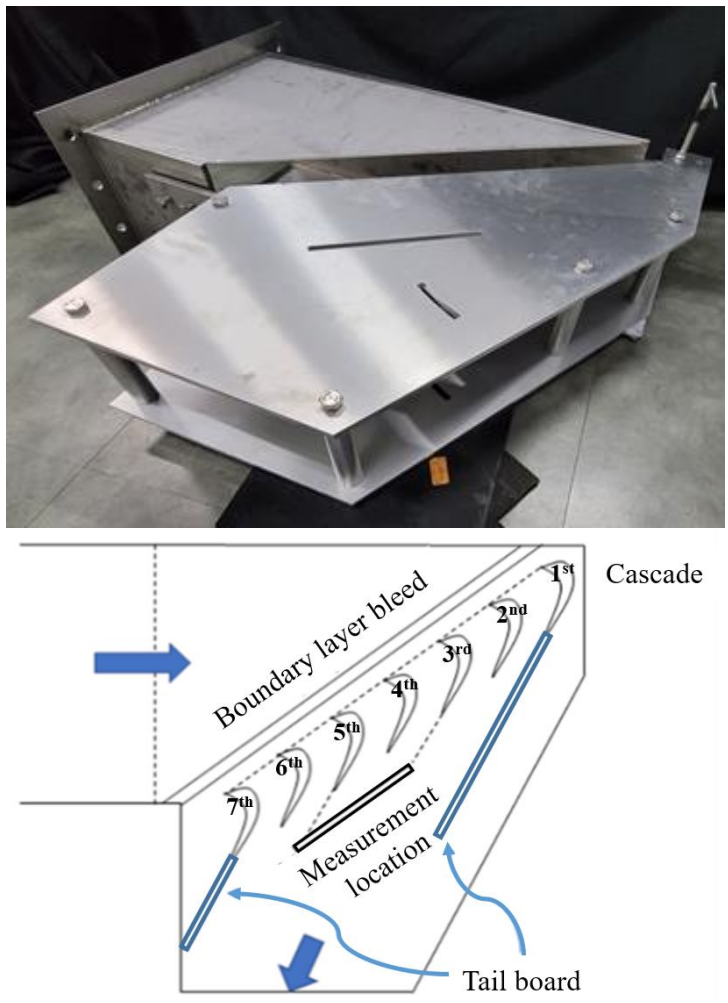

Fig. 2. Linear cascade

2.2. Experimental Conditions

Details of the blade geometry are given in Table 1. The tip has a flat face without any special features, and four different tip clearances were analyzed: 0%, 1.4%, 2.8%, and 4.2% span when the Reynolds number was 2.0 x 10^5. The blade tip section has a modular design, such that different height tips can be attached, making it possible to adjust the tip clearance economically and efficiently (Fig. 3). When the tip clearance was 2.8%, the Reynolds number was analyzed approximately 1.7 x 10^5, 2.0 x 10^5, and 2.3 x 10^5 based on blade exit velocity and chord length.

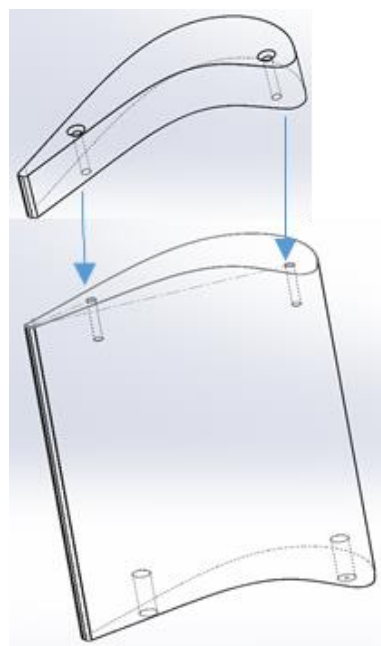

Fig. 3. Schematic of modular blade tip

Table 1. Blade geometry

Inlet blade angle (α)	53°
Outlet blade angle (β)	60°
Chord length (c)	103 mm
Span/c	1.75
Pitch/c	0.97
Number of blades	7
Tip clearance (τ/s)	0%, 1.4%, 2.8%, 4.2%
Reynolds # ($\times 10^5$)	1.7, 2.0, 2.3

2.3. Instrumentation

The measurement was carried out with a 5-hole probe mounted on a 2-axis translation stage. An L-shaped 5-hole probe with 3 mm head diameter from Vectoflow was used for the experiment and was connected to the Scanivalve DSA3217 pressure scanner. The measurement area was 176 mm in width and 170 mm in height, and 23 points in the pitch direction and 35 points in the span direction were measured, which includes roughly two passages from the third to fifth blade, as depicted in Fig. 2.

Fig. 4. 5-hole probe (top), 2-axis translation stage (left), and pressure scanner (right)

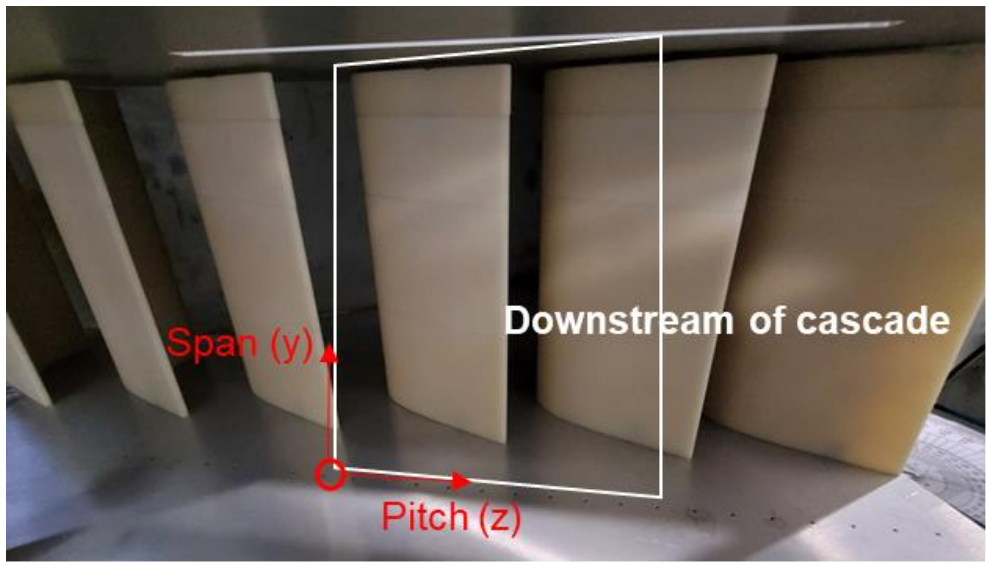

Fig. 5. 5-hole probe measurement area

2.4. Experimental Uncertainty

Uncertainty analysis was performed using the method suggested by Moffat [20]. The uncertainty of the 5-hole probe used in this study depends on measurement error of velocity and angle. Error evaluation was performed 210 times at 0.3 Mach number by Vectoflow. The standard deviation of the velocity magnitude, pitch angle, and yaw angle were 0.13 m/s, 0.13°, and 0.22°, respectively. The uncertainty of the total pressure loss coefficient was calculated using the equation below. A coverage factor of 2 was multiplied for 95% confidence level. The uncertainty is about 18% at for the 2.8% tip clearance, which is the base case of this study.

$$\delta Y = \left\{ \left(\frac{\delta P_{t,in}}{\frac{1}{2}\rho {V_{in}}^2} \right)^2 + \left(\frac{\delta P_{t,out}}{\frac{1}{2}\rho {V_{in}}^2} \right)^2 + \left(\frac{P_{t,in} - P_{t,out}}{\frac{1}{4}\rho {V_{in}}^3} \delta V \right)^2 \right\}^{\frac{1}{2}} \quad (1)$$

2.5. Static Pressure Periodicity

When the flow passes through the cascade, boundary layers are formed along the blade surfaces, and regions of high and low velocity magnitude appear repeatedly at the cascade exit due to this wake. The static pressure coefficient, which is defined below in Eq. (2), is plotted against the blade pitch in Fig. 6.

$$C_p = \frac{P_s - P_{s,\infty}}{\frac{1}{2}\rho {U_{in}}^2} \qquad (2)$$

A periodic trend is observed, which suggests that the central two passages can be utilized to obtain representative measurements of the flow.

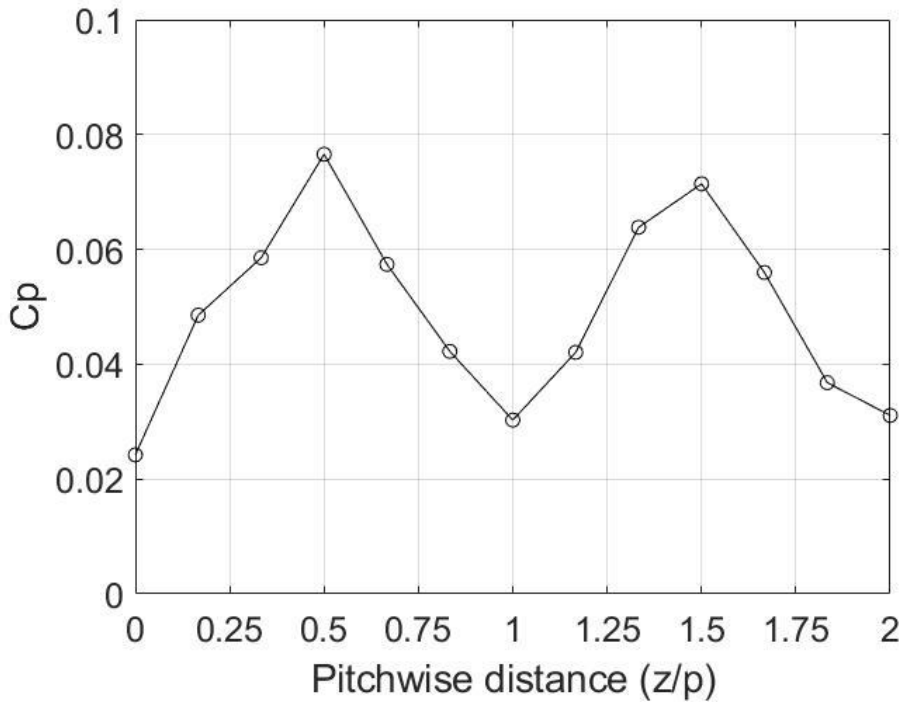

Fig. 6. Pressure coefficient distribution downstream of the turbine cascade

Chapter 3. Results of Tip Clearance Effects

The results section of this thesis consists of two parts. The first part examines flow characteristics and aerodynamic loss according to the change of tip clearance. This was previously published by Chung et al. (2022) [21], and the paper is given here in its entirety. The second part performed the same study according to the change of Reynolds number.

3.1. Downstream Flow Structure

Fig. 7 shows the in-plane secondary flow field at the exit plane of the blades. In the case of zero tip clearance (Fig. 7a), passage vortices can be observed toward the tip and hub. These passage vortices are formed due to boundary layer development along the outer casing and inner hub endwalls entering the cascade. The tip passage vortex results in strong upward flow toward the tip.

As the tip clearance increases for Fig. 7 (b) – (d), a tip leakage vortex is created, as the flow "leaks" from the pressure to suction side. As this vortex increases in strength, it eventually pushes the tip passage vortex away toward the exit of the neighboring blade.

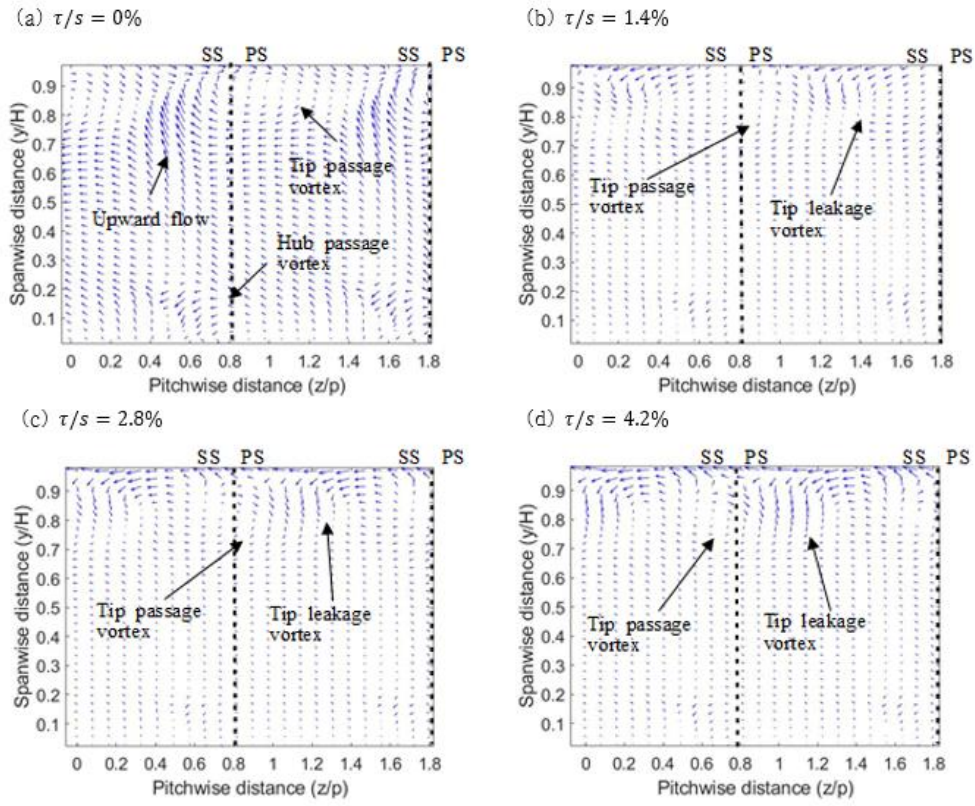

Fig. 7. Downstream flow structure with non-dimensional tip gap at (a) 0%, (b) 1.4%, (c) 2.8%, and (d) 4.2%

3.2. Streamwise Velocity Distribution

Fig. 8 shows the streamwise velocity contours at the blade exit plane. When there is no tip clearance (Fig. 8a), the wake structure along the span of the blade is prominent. This wake is caused by boundary layer development along both the pressure and suction surfaces of the blade. Because the exit flow angle is slightly smaller than the blade exit angle, this wake region is formed to the left of the suction side. The upper and lower streamwise velocity deficit regions within the wake correspond to the regions of strong secondary flow due to the tip and hub passage vortices from Fig. 7 (a), respectively. This velocity deficit is stronger than that of the inner hub and outer casing endwall regions, which are caused by endwall boundary layers. The streamwise velocity throughout the tip region (in the black oval) is fairly constant. Effects of the tip passage vortex can be observed in the black circle.

When there is a tip clearance, a sharp streamwise velocity deficit begins to occur in the tip region. As the tip clearance widens, the leakage flow intensifies, resulting in a significant decrease of the streamwise velocity and an enlargement of deficit area. This area also starts to merge with that of the tip passage vortex, as evidenced in Fig. 8 (d). Thus, the tip leakage vortex is starting to affect the passage vortex.

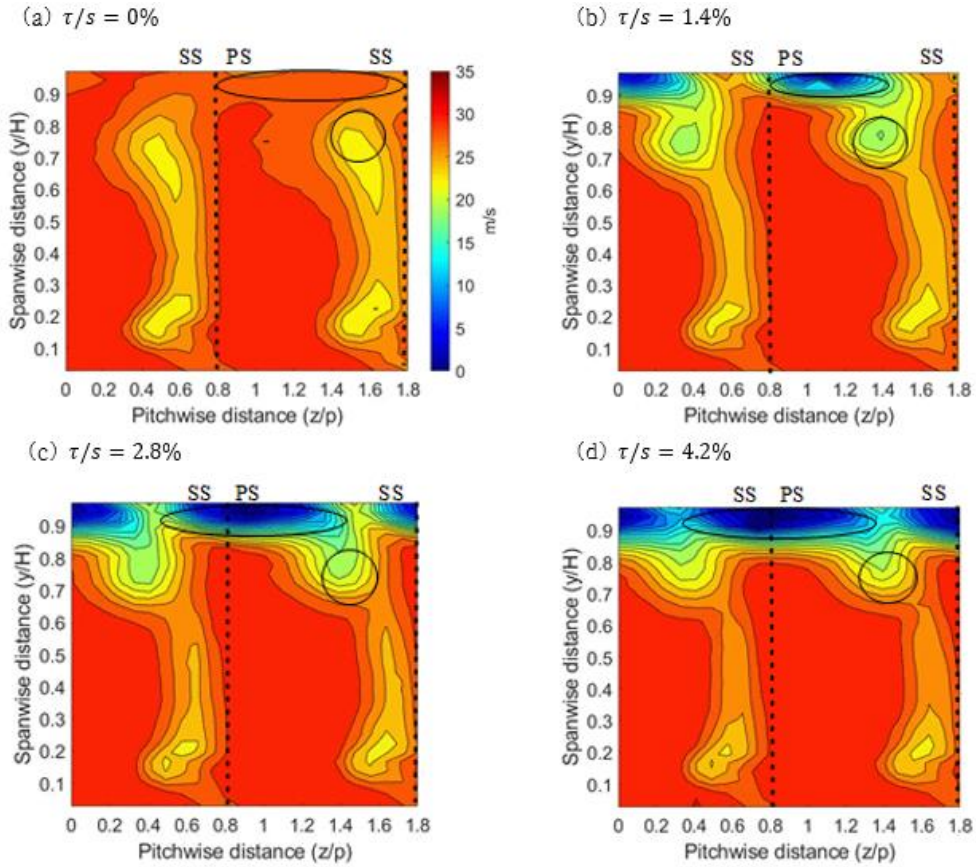

Fig. 8. Streamwise velocity distribution for non-dimensional tip gap at (a) 0%, (b) 1.4%, (c) 2.8%, and (d) 4.2%

3.3. Total Pressure Loss Coefficient Distribution

The aerodynamic loss coefficient is defined as the non-dimensional total pressure drop, as expressed in Eq. (3) below.

$$Y = \frac{P_{t,in} - P_{t,out}}{\frac{1}{2}\rho {U_{in}}^2} \qquad (3)$$

Fig. 9 depicts the loss coefficient contours at the blade exit plane. When there is no tip gap, profile loss occurs in the wake region of the blades (Fig. 9a), which coincides with the streamwise velocity deficit region in Fig. 8 (a).

As the tip clearance increases, tip leakage flow from the pressure side of the blade to the suction side results in significantly increased aerodynamic loss in the tip region.

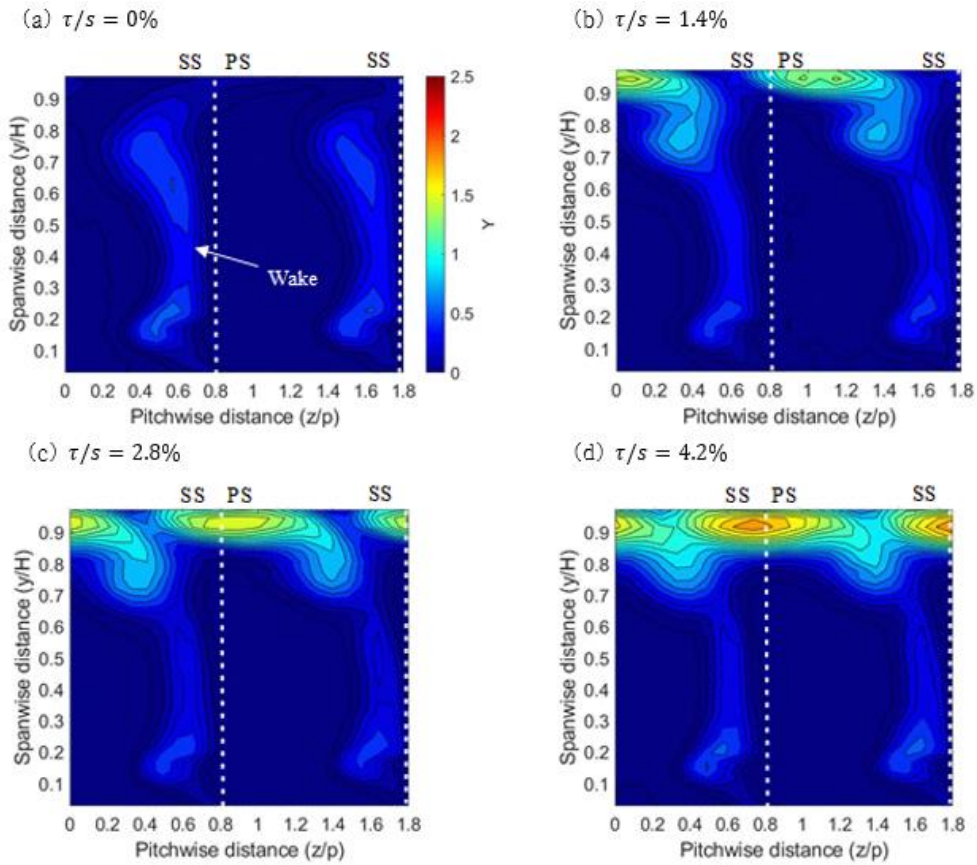

Fig. 9. Total pressure loss coefficient distribution for non-dimensional tip gap at (a) 0%, (b) 1.4%, (c) 2.8%, and (d) 4.2%

3.4. Pitch-wise Mass Averaged Loss Coefficient

The pitch-wise mass averaged loss coefficient is defined in Eq. (4) below. The pitch-wise mass averaged relative loss (with respect to the reference zero tip gap case) is defined in Eq. (5).

$$\bar{Y}_z = \frac{\int \rho U Y dz}{\int \rho U dz} \qquad (4)$$

$$\Delta_z = \bar{Y}_z - \bar{Y}_{z,0} \qquad (5)$$

Fig. 10 shows these pitch-wise mass averaged loss coefficients. The zero tip gap case in Fig. 10 (a) shows the loss due to the passage vortex in the hub area (near y/H = 0.2), profile loss in the mid-span area (roughly 0.3 < y/H < 0.6), and loss due to the passage vortex in the tip area (near y/H = 0.7).

As the tip gap is increased, the loss near the tip (y/H > 0.7) increases rapidly. For the non-dimensional tip gap of 1.4%, effects of the tip passage vortex loss can still be partially seen, but beyond 1.4% the tip clearance loss is dominant compared to the other losses, and reaches a value about tenfold for the 4.2% case compared to the zero tip gap case.

Fig. 10 (b) displays the relative loss with respect to the zero tip gap case. It can be clearly seen that an increase in tip clearance causes a marked increase in total pressure loss, resulting in a significant reduction of aerodynamic performance at the tip. Although this does not affect the hub passage vortex loss, it does

cause a reduction in tip passage vortex loss, evidenced by both figures at $y/H = 0.6$.

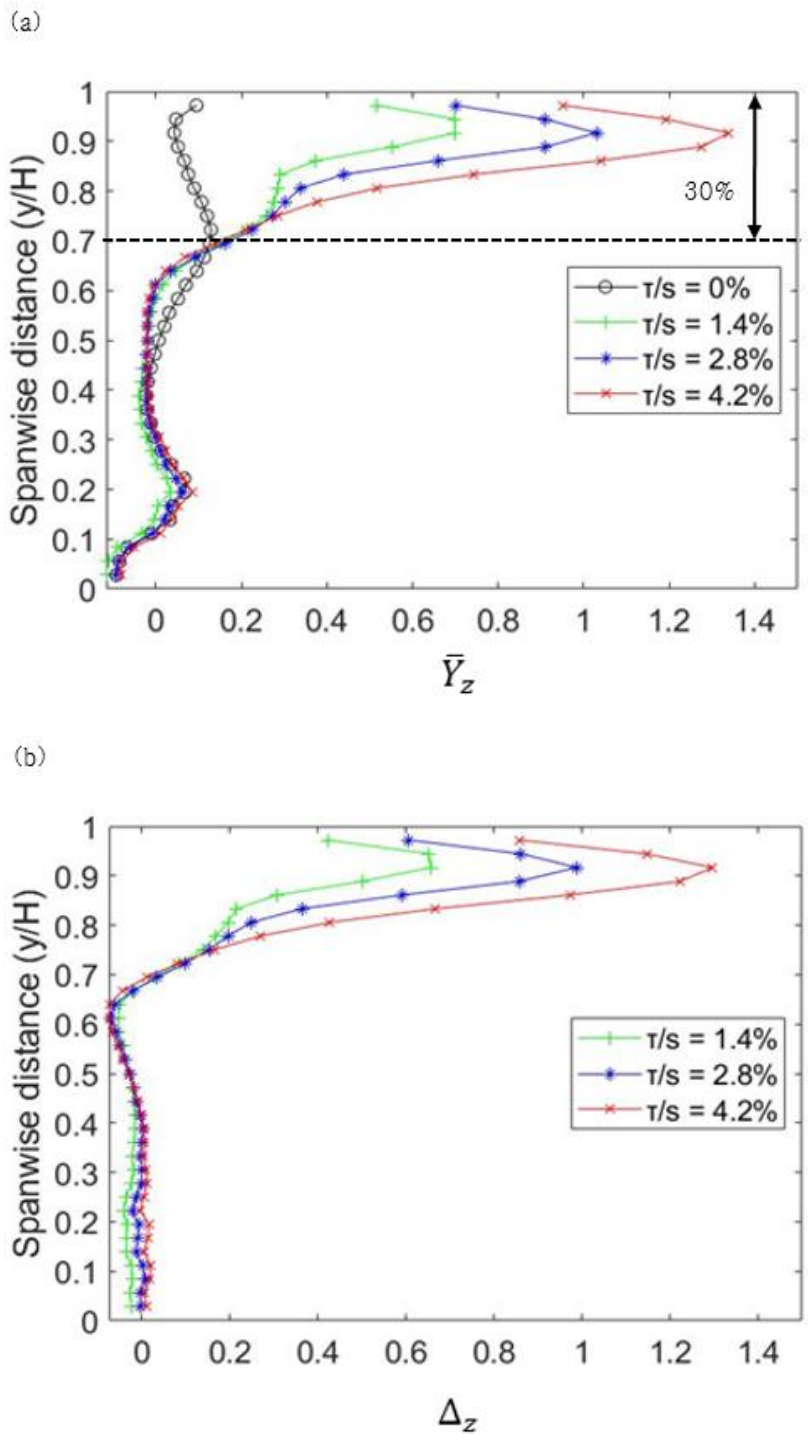

Fig. 10. (a) Pitch−wise mass averaged loss coefficient,
(b) relative loss with tip clearance

3.5. Overall Mass Averaged Loss Coefficient

The overall mass averaged loss coefficient is given in Eq. (6), and the overall relative loss (with respect to the reference zero tip gap case) is defined in Eq. (7).

$$\bar{Y} = \frac{\int\int \rho UY dy dz}{\int\int \rho U dy dz} \qquad (6)$$

$$\Delta = \bar{Y} - \bar{Y}_0 \qquad (7)$$

This measured relative loss and predicted loss models applied to this study are plotted in Fig. 11. Table 2 shows various predicted loss models of the tip clearance loss. The overall loss and predicted loss increase quite linearly with tip clearance. Among the various presented loss models, the result of this study were quite consistent with Yaras and Sjolander [8]. Table 3 quantitatively summarizes the measured overall loss and predicted loss. Similarly, it can be seen that the measured loss and the predicted loss of Yaras and Sjolander [8] are in good agreement.

Table 2. Correlations of tip clearance loss

Loss model	Tip clearance loss (Δ)
Ainley and Mathieson [6]	$0.5\left(\frac{k}{h}\right)\left(\frac{c}{s}\right)^2 C_L\left(\frac{\cos^2\alpha_2}{\cos^3\alpha_m}\right)\left(\frac{Re}{2\times10^5}\right)^{-0.2}$
Dunham and Came [7]	$0.47\left(\frac{c}{h}\right)\left(\frac{k}{c}\right)^{0.78}\left(\frac{c}{s}\right)^2 C_L^2\left(\frac{\cos^2\alpha_2}{\cos^3\alpha_m}\right)$
Yaras and Sjolander [8]	$2K_E C_D\left(\frac{k}{h}\right)\left(\frac{c}{s}\right) C_L^{1.5}\left(\frac{\cos^2\alpha_2}{\cos^3\alpha_m}\right)$

Note: k: tip clearance

h: blade height

c: chord length

s: pitch

C_L: lift coefficient

C_D: discharge coefficient

K_E: constant related to loading distribution

α_2: exit flow angle

α_m: mean flow angle

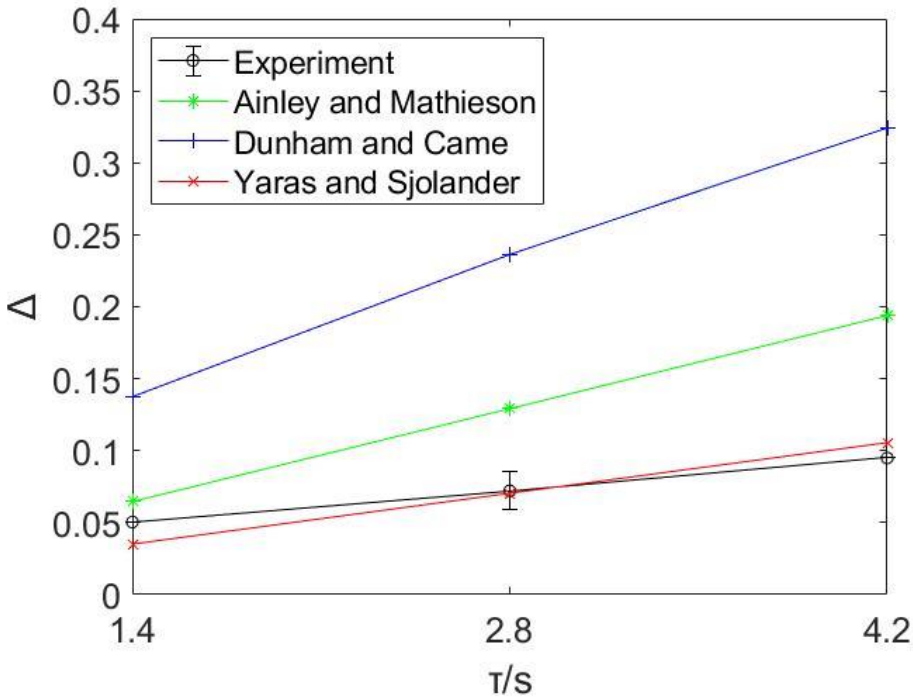

Fig. 11. Overall relative loss and loss models with tip clearance

Table 3. Values of tip clearance loss with tip clearance

Loss model	Tip clearance loss (Δ)		
	$\tau/s = 1.4\%$	$\tau/s = 2.8\%$	$\tau/s = 4.2\%$
Experiment	0.0504	0.0721	0.0949
Ainley and Mathieson [6]	0.0646	0.1292	0.1939
Dunham and Came [7]	0.1375	0.2363	0.3243
Yaras and Sjolander [8]	0.0351	0.0704	0.1056

Chapter 4. Results of Reynolds Number Effects

4.1. Downstream Flow Structure

Fig. 12 shows the in-plane secondary flow field at the exit plane of the blades. In each Reynolds number at zero tip clearance, the same flow phenomenon as shown in Fig. 7 (a) was observed, and no significant change occurred.

Likewise, as the Reynolds number increases for Fig. 12, there was little change in the downstream flow structure. Each flow phenomenon was observed at a similar position and intensity in the in-plane secondary flow field with a 2.8% tip clearance shown in Fig. 7 (c).

(a) Re = 1.7 x 10^5

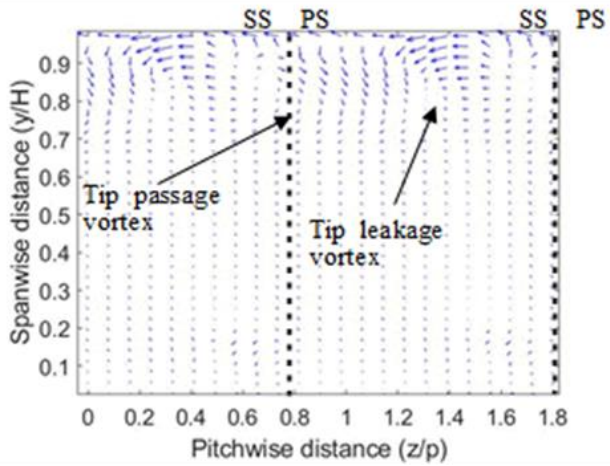

(b) Re = 2.0 x 10^5

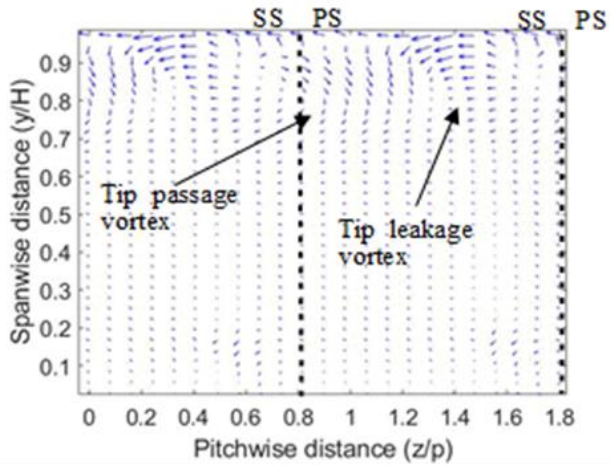

(c) Re = 2.3 x 10^5

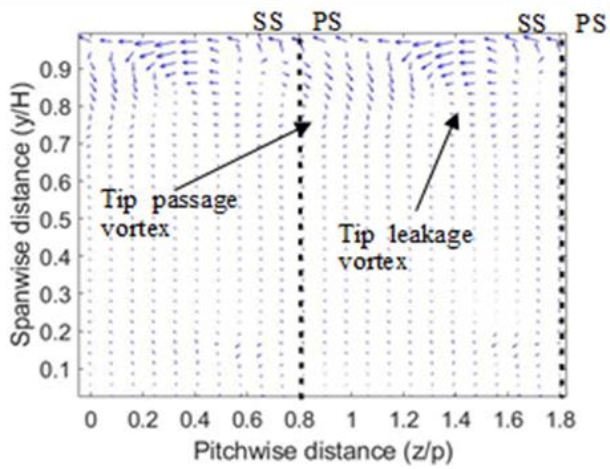

Fig. 12. Downstream flow structure with Reynolds number at (a) 1.7 x 10^5, (b) 2.0 x 10^5, and (c) 2.3 x 10^5

4.2. Streamwise Velocity Distribution

Fig. 13 shows the streamwise velocity contours at the blade exit plane. When there is no tip clearance in each case, the wake structure along the span of the blade is prominent like Fig 8 (a). In other words, there has been little change in its form. But, of course, the streamwise velocity appeared faster as the Reynolds number increased.

When there is a tip clearance, a sharp streamwise velocity deficit begins to occur in the tip region. As the Reynolds number increases, this deficit was similar in shape and magnitude in the tip region, but the streamwise velocity increased overall in the rest of the tip region (Fig. 13). In each case, the velocity decrease by leakage flow, passage vortex, and wake was confirmed.

(a) Re = 1.7 x 10^5

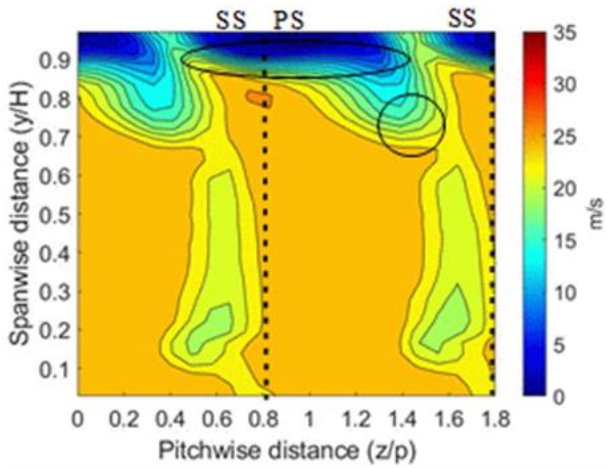

(b) Re = 2.0 x 10^5

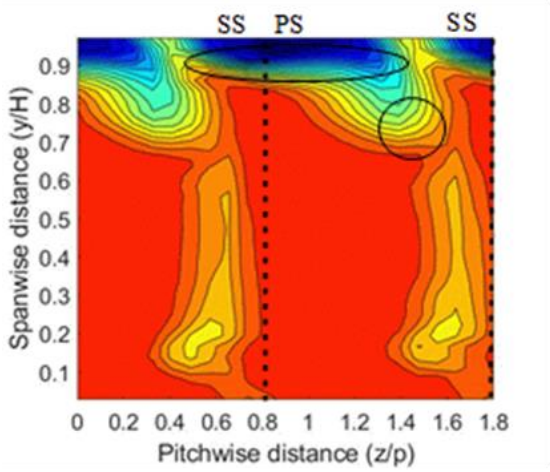

(c) Re = 2.3 x 10^5

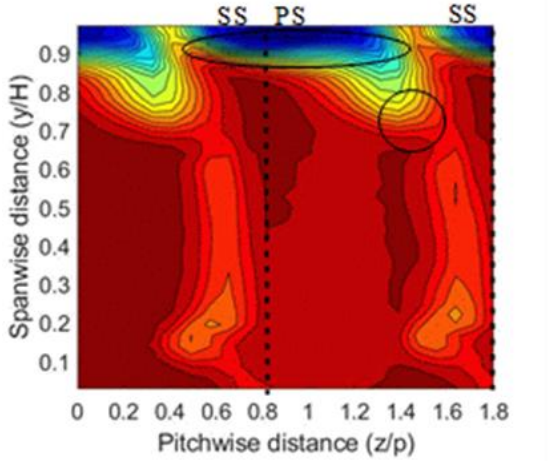

Fig. 13. Streamwise velocity distribution for Reynolds number at (a) 1.7 x 10^5, (b) 2.0 x 10^5, and (c) 2.3 x 10^5

4.3. Total Pressure Loss Coefficient Distribution

The aerodynamic loss coefficient is defined as the non-dimensional total pressure drop, as expressed in Eq. (3). Fig. 14 depicts the loss coefficient contours at the blade exit plane. When there is no tip clearance in each case, profile loss occurs in the wake region of the blades like Fig. 9 (a), which coincides with the streamwise velocity deficit region in Fig. 8 (a). Its shape and magnitude remained almost unchanged.

As shown in Fig 14, tip leakage flow from the pressure side of the blade to the suction side results in significantly increased aerodynamic loss in the tip region. However, despite the increase in Reynolds number, the contour of the total pressure loss coefficient did not show significant change. In each case, the total pressure loss by leakage flow, passage vortex, and wake was confirmed.

(a) Re = 1.7 x 10^5

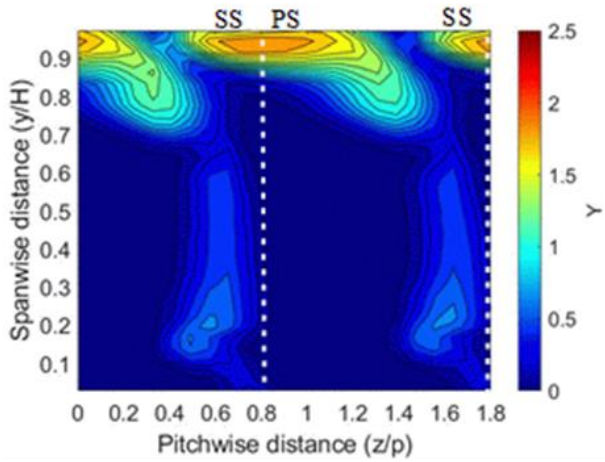

(b) Re = 2.0 x 10^5

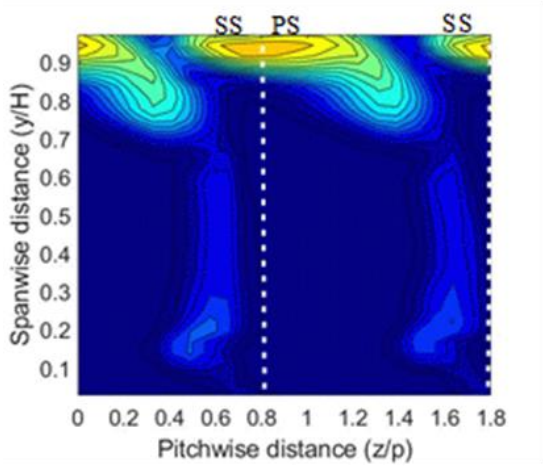

(c) Re = 2.3 x 10^5

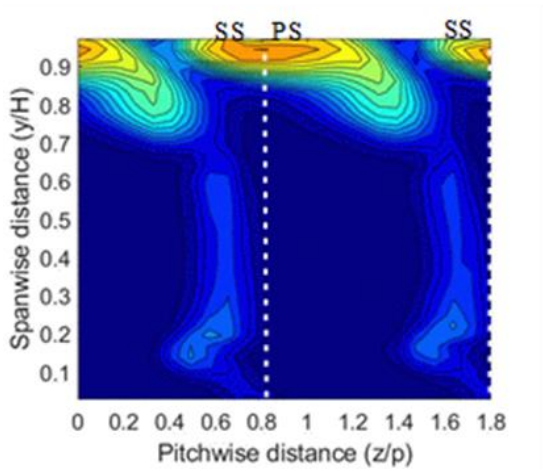

Fig. 14. Total pressure loss coefficient distribution for Reynolds number at (a) 1.7 x 10^5, (b) 2.0 x 10^5, and (c) 2.3 x 10^5

4.4. Pitch-wise Mass Averaged Loss Coefficient

The pitch-wise mass averaged loss coefficient is defined in Eq. (4). The pitch-wise mass averaged relative loss (with respect to the reference zero tip gap case) is defined in Eq. (5). When there was zero tip gap according to each Reynolds number, losses along the span appeared same as mentioned in Fig. 10 (a).

Fig. 15 displays the pitch-wise mass averaged relative loss with respect to the zero tip gap case of each Reynolds number. It can be clearly seen that the presence of tip clearance causes a marked increase in total pressure loss regardless of the Reynolds number ($y/H > 0.7$). This dominant loss results in a significant reduction of aerodynamic performance at the tip. However, there was no significant modification in the loss according to the change of the Reynolds number. This can be said to verify the reason why the Reynolds number was not included in most of the various tip clearance loss correlations derived from previous studies.

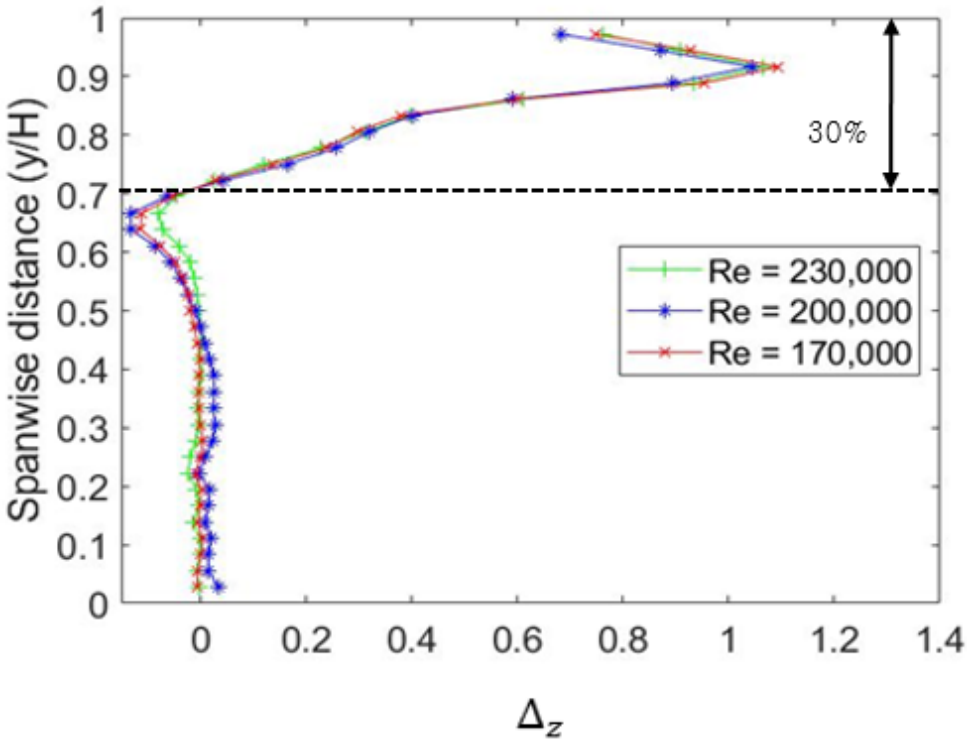

Fig. 15. Relative loss with Reynolds number

4.5. Overall Mass Averaged Loss Coefficient

The overall mass averaged loss coefficient is given in Eq. (6), and the overall relative loss (with respect to the reference zero tip gap case) is defined in Eq. (7). This measured relative loss and predicted loss models applied to this study are plotted in Fig. 16. The overall loss and predicted loss were fairly constant with little change depending on the Reynolds number. In the correlation of Ainley and Mathieson [6] as in the Table 2, since the Reynolds number acts as a variable, there is a slight change, but it is insignificant for the Reynolds number over 2.0×10^5. However, since the rest of the correlations are independent of the Reynolds number, they indicate a completely constant loss. Among these various presented loss models, the result of this study were quite consistent with Yaras and Sjolander [8]. Table 3 quantitatively summarizes the measured overall loss and predicted loss. Similarly, it can be seen that the measured loss and the predicted loss of Yaras and Sjolander [8] are in good agreement.

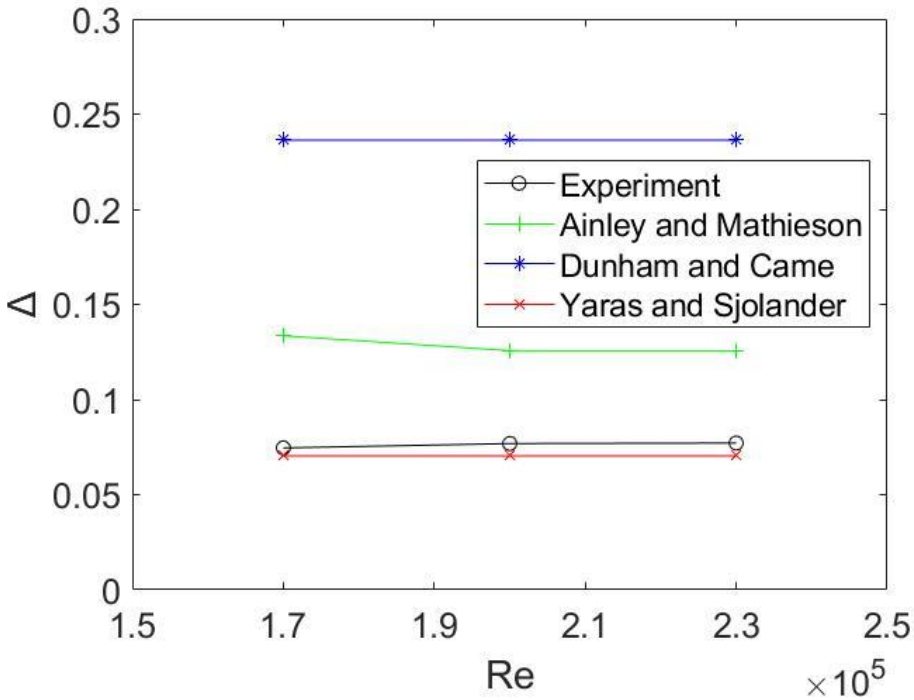

Fig. 16. Overall relative loss and loss models with Reynolds number

Table 4. Values of tip clearance loss with Reynolds number

Loss model	Tip clearance loss (⊿)		
	Re = 1.7 x 10^5	Re = 2.0 x 10^5	Re = 2.3 x 10^5
Experiment	0.0746	0.0768	0.0771
Ainley and Mathieson [6]	0.1335	0.1257	0.1256
Dunham and Came [7]	0.2363	0.2363	0.2363
Yaras and Sjolander [8]	0.0704	0.0704	0.0704

Chapter 5. Conclusions

In this study, the complex flow structure within a gas turbine rotor was investigated, and its effects on aerodynamic loss was quantified. A turbine linear cascade was constructed, and periodicity of the flow downstream of the cascade was confirmed. Using a 5-hole probe, velocity and pressure measurements were obtained both with and without tip clearance. The total pressure loss coefficient field for each case was measured for various tip clearances and Reynolds numbers, and the aerodynamic loss was evaluated. In addition, the preceding correlations of tip clearance loss were applied to this study, and the results were compared and analyzed.

As the tip clearance increased from 0% to 4.2% of blade span at 2.0×10^5 Reynolds number, the influence of the tip leakage vortex increased and widened to the tip passage vortex region. Because of the interference of the tip leakage flow with the main flow, the total pressure loss increases significantly by tenfold in the 70 - 100% blade span region for the 4.2% span tip clearance case. The overall aerodynamic loss also increases linearly with tip clearance.

On the other hand, although the Reynolds number increased from 1.7×10^5 to 2.3×10^5 based on blade exit velocity and chord length at 2.8% tip clearance, the flow characteristics were similar to the results derived from the 2.8% tip clearance conducted in the experiment according to the tip clearance. The overall

aerodynamic loss also remained almost constant for various Reynolds numbers. In this respect, the influence of the Reynolds number on the same tip clearance was insignificant.

Acknowledgements

This study was carried out as part of the project of The UAV Turbine Research Center supported by the Defense Acquisition Program Administration and the Agency for Defense Development.

Bibliography

[1] Bindon J.P., The Measurement and Formation of Tip Clearance Loss. Journal of Turbomachinery, 1989, Vol. 111.

[2] Nho Y.C., Park J.S., Lee Y.J., and Kwak J.S., Effects of turbine blade tip shape on total pressure loss and secondary flow of a linear turbine cascade. International Journal of Heat and Fluid Flow, 2012, Vol. 33, pp. 92-100.

[3] Wang T., Xuan Y., and Han X., The effects of tip gap variation on transonic turbine blade tip leakage flow based on VLES approach. Aerospace Science and Technology, 2021, Vol. 111, 106542.

[4] Yamamoto A., Interaction mechanisms between tip leakage flow and the passage vortex in a linear turbine rotor cascade. Journal of Turbomachinery, 1988, Vol. 110.

[5] Yamamoto A., Production and development of secondary flows and losses in two types of straight turbine cascades: Part 2 - A rotor case. Journal of Turbomachinery, 1987, Vol. 109.

[6] Ainley D.G., and Mathieson G.C.R., A method of performance estimation for axial flow turbines. British ARC, 1951, R&M 2974.

[7] Dunham J., and Came P.M., Improvements to the Ainley-Mathieson method of turbine performance prediction. Journal of Engineering for Power, 1970, 92, pp. 252-256.

[8] Yaras M.I., and Sjolander S.A., Prediction of tip-leakage

losses in axial turbines. Journal of Turbomachinery, 1992, 114, pp. 204-210.

[9] Jonas Persson, 1D Turbine Design Tool Validation and Loss Model Comparison: Performance Prediction of a 1-stage Turbine at Different Pressure Ratios. KTH School of Industrial Engineering and Management, Master of Science Thesis, 2015.

[10] Sjolander S.A., and Cao D., Measurements of the flow in an idealized turbine tip gap. Journal of Turbomachinery, 1995, Vol. 117.

[11] Williams R., Gregory-Smith D., He L., and Ingram G., Experiments and computations on large tip clearance effects in a linear cascade. Proceedings of ASME Turbo Expo, 2008.

[12] Matsunuma T., Effects of Reynolds number and freestream turbulence on turbine tip clearance flow. Journal of Turbomachinery, 2006, Vol. 128.

[13] Bi Z., Shao X., and Zhang L., Numerical study of tip leakage vortex around a NACA0009 hydrofoil. Journal of Fluids Engineering, 2021, Vol. 143, 051203.

[14] Yaras M. I., Sjolander S. A., Kind R. J., Development of the Tip-Leakage Flow Downstream of a Planar Cascade of Turbine Blades: Vorticity Field. Journal of Turbomachinery, 1990, Vol 112.

[15] Yaras M. I., Sjolander S. A., Kind R. J., Effects of Simulated Rotation on Tip Leakage in a Planar Cascade of Turbine Blade: Part 1 - Tip Gap Flow. Journal of Turbomachinery, 1992, Vol 114.

[16] Yaras M. I., Sjolander S. A., Kind R. J., Effects of

Simulated Rotation on Tip Leakage in a Planar Cascade of Turbine Blade: Part 2 - Downstream Flow Field and Blade Loading. Journal of Turbomachinery, 1992, Vol 114.

[17] Tallman J., and Lakshminarayana B., Numerical simulation of tip leakage flows in axial flow turbines, with emphasis on flow physics: Part 1 – Effect of tip clearance height. Journal of Turbomachinery, 2001, Vol. 123.

[18] Tallman J., and Lakshminarayana B., Numerical Simulation of Tip Leakage Flows in Axial Flow Turbines, With Emphasis on Flow Physics: Part II—Effect of Outer Casing Relative Motion. Journal of Turbomachinery, 2001, Vol. 123.

[19] Dianliang Yang, Xiaobing Yu, and Zhenping Feng, Investigation of Leakage Flow and Heat Transfer in a Gas Turbine Blade Tip with Emphasis on the Effect of Rotation. Journal of Turbomachinery, 2010, Vol. 132, 041010.

[20] Moffat R.J., Describing the Uncertainties in Experimental Results. Experimental Thermal and Fluid Science, 1988, 1(1), pp. 3-17.

[21] Chung J.M., Baek S.C., and Hwang W.T., Experimental Investigation of Aerodynamic Performance due to Blade Tip Clearance in a Gas Turbine Rotor Cascade. Journal of Thermal Science, 2022, Vol 31, No. 1, pp. 173-178.

Abstract

본 연구에서는 가스터빈 로터 내부의 복잡한 유동 구조가 공력 손실에 어떠한 영향을 미치는지 조사하였다. 덮개가 없는 선형 터빈 캐스케이드를 구축하였고 5공 프로브를 사용하여 속도장 과 압력장을 측정하였다. 팁 간극과 레이놀즈 수의 영향을 설명하기 위해 각 경우에 대한 전압력장을 조사하여 전반적인 공력 손실을 평가하였다. 팁 간극은 블레이드 스팬의 0%에서 4.2%까지, 코드 길이 기반 레이놀즈 수는 1.7×10^5에서 2.3×10^5까지 변화시켰다.

팁 간극이 없는 경우, 허브 및 팁 통로 와류와 함께 블레이드 후연의 하류 후류가 관찰되었다. 이러한 유동 구조로 인해 블레이드 스팬의 중심에서의 형상 손실과 허브 및 팁으로 향하는 통로 와류와 관련된 손실이 발생하였다. 팁 간극이 증가함에 따라 팁 누설 와류가 형성되고 점차 강해져 결국 팁 통로 와류를 변화시켰다. 2차 팁 누설 유동과 주 유동의 간섭으로 인해 흐름 방향 속도는 감소하는 반면, 전압력 손실은 4.2% 팁 간극의 경우에 팁 방향으로 블레이드 스팬 영역의 마지막 30%에서 10배로 크게 증가하였다.

또한 전반적인 공력 손실은 팁 간극에 따라 선형적으로 증가하는 것으로 관찰되었다. 한편, 레이놀즈 수에 의한 영향은 흐름 방향 속도를 증가시켰으나 유동 구조와 공력 손실의 변화는 미미하였다.

주요어 : 가스터빈, 로터 캐스케이드, 공력 손실, 팁 간극, 레이놀즈 수

학번 : 2020-25852